Caspian Journal of Environmental Sciences
Online ISSN: 1735-3866
Print ISSN: 1735-3033

Highly adsorption of alginate/bentonite impregnated TiO_2 beads for wastewater treatment: Optimization, kinetics, and regeneration studies

Zainab D. Alhattab[1], Aseel M. Aljeboree[2], Mohammed Abed Jawad[3], Fatime Satar Sheri[4], Ahmed Kareem Obaid Aldulaim[5], Ayad F. Alkaim[2*]

1. Ministry of Interior Affairs, Babylon Police Command, Criminal Evidence Investigation Department, Iraq
2. Department of Chemistry, College of Sciences for W, University of Babylon, Hilla, Iraq
3. Department of Medical Laboratories Technology, AL-Nisour University College, Baghdad, Iraq
4. National University of Science and Technology, Dhi Qar, Iraq
5. Department of Pharmacy, Al-Zahrawi University College, Karbala, Iraq

** Corresponding author's Email: alkaimayad@gmail.com*

ABSTRACT

In this work, we prepared an eco-friendly, simple, stable new adsorbent SA-Bn-TiO_2 NPs hydrogel and Comparative between SA-Bn-TiO_2 NPs, SA-Bn, and TiO_2 NPs surfaces as adsorbents. The best results of the percentage of removal (E%) of two pollutants including Amoxicillin (AMX) and 4-chlorophenol (CPH) arranged in the order of increasing as SA-Bn-TiO_2 NPs > SA-Bn > TiO_2 NPs. The good results of the percentage of removal (E%) of SA-Bn-TiO_2 NPs were 87.56% and 82.56 for AMX and CPH at the same order. Kinetics adsorption models of two pollutants on SA-Bn-TiO_2 NPs was studied and modelled utilizing three adsorptions kinetic. The classification of the kinetic models according to the simulation of the adsorption study is pseudo first order > pseudo-second order > chemisorption. Recyclability and desorption studies indicated the better reusing performance of the prepared composite. Based on the results, the prepared nano-composites can be useful as a promising, cost-effective, environmentally friendly, and efficient material for pollutant decontamination. Studies was carried out utilizing several desorption agents at various concentrations (0.01, 0.05 and 0.1 N) including HNO_3, H_2SO_4, HCl, NaOH, H_3PO_4, ethanol, acetone and water. The SA-Bn-TiO_2 NPs was regeneration with 100% using water.

Keywords: Hydrogel, Recyclability, Amoxicillin, Chlorophenol, Kinetics model.
Article type: Research Article.

INTRODUCTION

Adsorption is a fast phenomenon of negative separation of adsorbate from phase aqueous/gaseous on a solid phase (Ardizzone *et al.* 1993; Wared & Radia 2021). Adsorption happens among two phases in transfer pollutants from one phase to second. It is considered to be a complex phenomenon and rely especially on the surface chemistry or nature of the adsorbate, adsorbent, and the system conditions in among the two phases. Adsorption methods offer the utmost economical and effective treatment way for the removal of pollutants from waste water. The process is often carried out in a batch mode (Ho & McKay 1994), via adding an adsorbent to a vessel having contaminated water, stirring the mixture for a sufficient time, then letting the adsorbent settle, and drawing off the cleansed water (Al Mashhadani *et al.* 2021; Karim & Radia 2022; Nasir *et al.* 2022; Saleh Ibrahim *et al.* 2022). The adsorbate is the material that is presence removed from the liquid phase. The adsorbents are the solid, gas and liquid phases onto which the adsorbate accumulates. The term adsorption is too used to portray two type of forces of interaction among adsorbent and adsorbate. These interaction forces are broadly depicted as chemi-sorption (chemical adsorption), and physi-sorption (Rouquerol *et al.* 1999; Aljeboree & Alkaim 2019; physical adsorption; Al Mashhadani *et al.* 2021).

 Received: Dec. 03, 2022 Revised: March 19, 2023 Accepted: May 25, 2023
DOI: 10.22124/CJES.2023.6943

Publisher: University of Guilan,

MATERIALS AND METHODS

Experimental part

Determination of optimum calibration curves of Amoxicillin (AMX) and 4-Chlorophenol (CPH)

A stander solution (1000 mg L^{-1}) was prepared via dissolving 1.0 g AMX and CPH in 1000 mL distilled water (DW). The calibration curve of several concentrations of these two drugs were prepared in serial dilutions (2-100 mg L^{-1}). In addition, absorbance was measured at the λ max for them. The calibration curves of AMX and CPH are shown in Fig. 1.

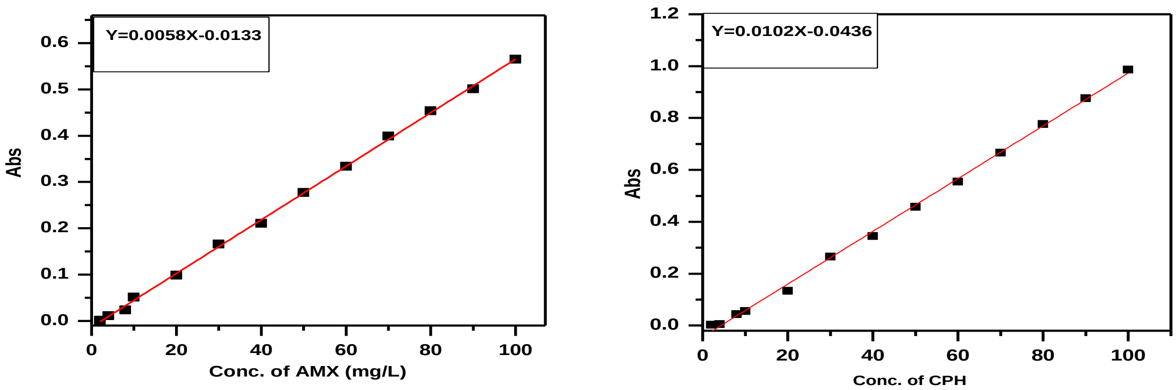

Fig. 1. Calibration curve for Amoxicillin (AMX) and 4-Chlorophenol (CPH).

In order to estimate the precision and accuracy of the way, solutions contained ten several concentrations. The measured detection limit (LOD), limits of Quantitation's (LOQ), RSD (%) and SD are presented in Table 1.
The LOD and LOQ for the proposed method were calculated using equations 1 and 2.

$$\mathrm{LOD} = \frac{3\ \mathrm{S.D}}{\mathrm{b}} \qquad (1)$$

The limits of Quantitation's (LOQ) was experimentally calculated using equation 2:

$$\mathrm{LOQ} = \frac{10\ \mathrm{SD}}{\mathrm{b}} \qquad (2)$$

SD is the standard deviation and *b* is the sensitivity, namely the slope of the calibration graph.

Table 1. Statistics data of calibration for several concentrations of Amoxicillin (AMX) and 4-Chlorophenol (CPH).

Parameters	**Proposed Method AMX**	**Proposed Method CPH**
λ_{max} (nm)	272	270
Beer's law limit (μg mL^{-1})	2–100	2-100
Regression equation	(Y = m X + C) Y= 0.0058X - 0.0133	(Y = m X + C) Y = 0.0102X - 0.0436)
Slope (m)	0.0058	0.0102
Intercept (C)	-0.0133	-0.0436
Correlation coefficient (r^2)	0.9993	0.9985
Color	Colorless	Colorless
LOD (μg mL^{-1})	1.027×10^{-4}	1.026×10^{-4}
LOQ (μg mL^{-1})	3.344×10^{-4}	3.422×10^{-4}
Relative standard deviation, RSD (%)	83.51	87.77
standard deviation (SD)	0.1986	0.349
Molar absorptivity (L/mol.cm)	2.119×10^{3}	1.311×10^{3}
Sandal's sensitivity (μg cm^{-1})	0.172×10^{-6}	9.8×10^{-8}

Adsorbent regeneration experiments

In order to investigate reusability of the adsorbents, 0.5 g SA-Bn-TiO_2 NPs adsorbent was added into 100 mL of each of the two pollutants (AMX and CPH) at the concentration of 500 mg L^{-1}, 30 °C and pH 6.0 to achieve saturated adsorption. The SA-Bn-TiO_2 NPs was regenerated in excess desorption studies utilizing several desorption agents at the concentrations of 0.01, 0.05 and 0.1 N such as HCl, H_2SO_4, H_3PO_4, HNO_3, NaOH, ethanol, acetone and water to regenerate anionic binding sites and finally washed with excess DW prior to use in the next adsorption cycle. An regenerate cycle was repeated 6 cycles utilizing 100 mL of pollutant solution at the concentration of 500 mg L^{-1}, 30 ºC and pH 6.0.

Removal of Pollutants (Dyes, pharmaceutical, and phenol compound) using SA-Bn-TiO_2 NPs

A real sample (100 mL) of pollutants containing phenol (PH), 4-Clorophenole (CPH), Amoxicillin (AMX), phenylephrine hydrochloride (PHE), Tetracycline (TC), Paracetamol (PR), Vitamin B_6 (pyridoxine), riboflavin (RF), Crystal Violet (CV), Methylene Blue (MB), Congo red (CR), Brilliant Blue (BB), Direct yellow (DY) with a riffle concentration were added in Erlenmeyer flask using 0.05 g SA-Bn-TiO_2 NPs, afterward the mixture were placed in a shaker water bath for one hour.

RESULTS AND DISCUSSION

Characterization of adsorbents surfaces

FESEM made used to study the morphology of hydrogel before and after AMX and CPH adsorption as shown in Fig.2. Through the results shown in Fig. 3a, the surface is rough and contains white particles, evidence of the tolerance of titanium oxide on the surface of the prepared hydrogel. In Figs. 2b and 2c after the adsorption process, it was observed that most of the effective sites of the surface were filled with the occurrence of many irregular zigzags on the surface, evidence of successful adsorption (Aljeboree *et al.* 2019; Karim & Radia 2022). The technique of TEM was also studied after loading titanium oxide on the prepared hydrogel as shown in Fig. 2d.

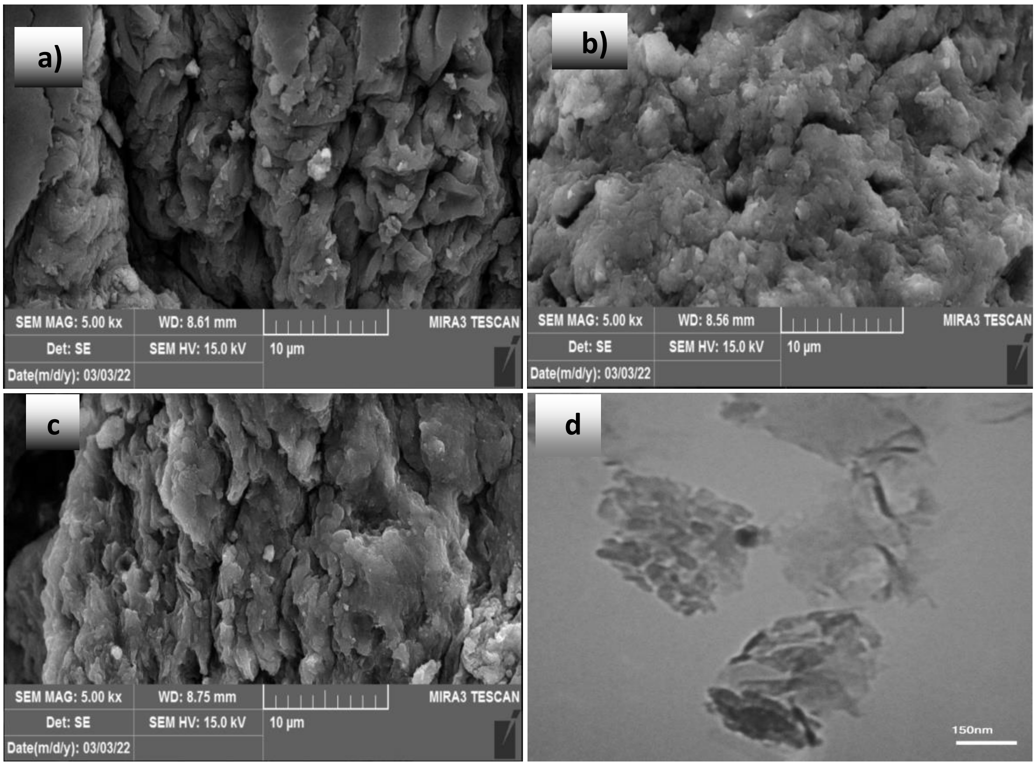

Fig. 2. FE-SEM images of (a) SA-Bn-TiO_2 NPs; (d) AMX loaded SA-Bn-TiO^2 NPs; (e) CPH loaded SA-Bn-TiO_2 NPs; and TEM images of (a) SA-Bn-TiO_2 NPs.

Removal of pollutants Using SA-Bn-TiO_2 NPs

A laboratory samples (100 mL) of pollutants (drugs, dyes and chemical compounds) with a refry concentrations were utilized in this experiment, followed by adding 0.05 g of SA-Bn-TiO_2 NPs to Erlenmeyer flask and placing in a shaker water bath for one hour, afterward, separating via centrifuge and measuring the remaining concentration via utilizing UV-Vis spectrophotometer (Xiong *et al.* 2020; Shoaib Nawa *et al*. 2022). The result are shown in Figs. 3a-c.

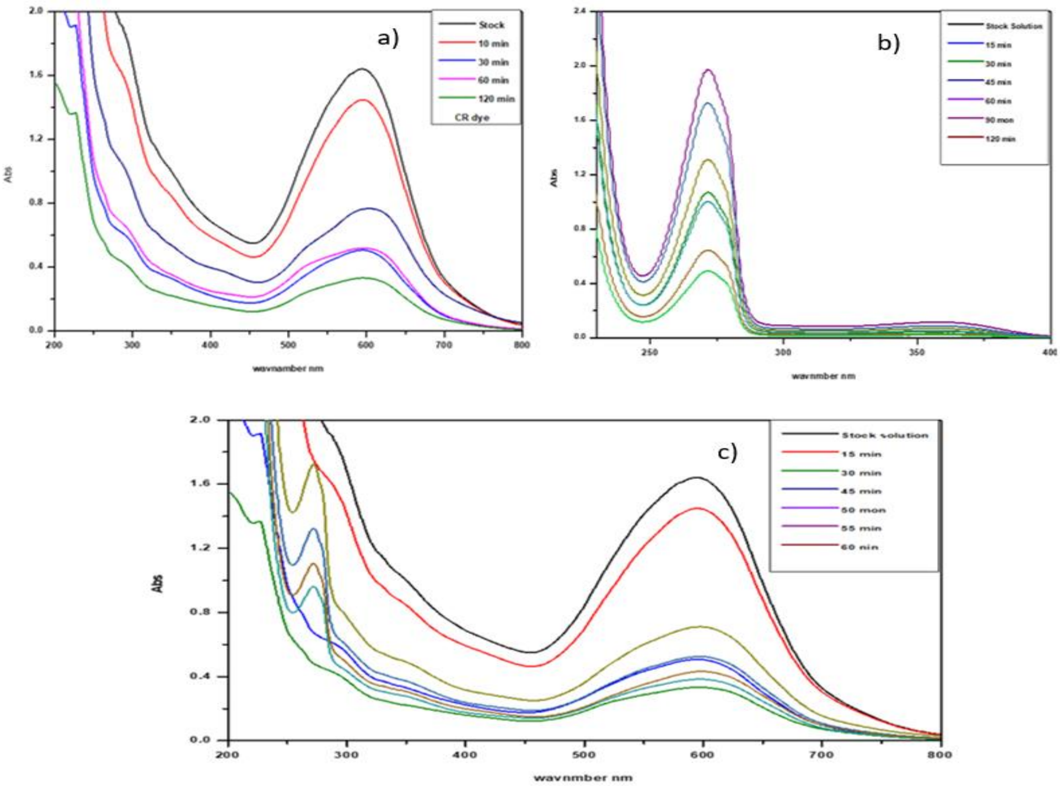

Fig. 3. Spectrum of removal several pollutants a) only dyes, b) only drugs c) dyes and drug using SA-Bn-TiO_2 NPs.

Regeneration of SA-Bn-TiO_2 NPs

The reactivated of hydrogels, after sorption, is one of the important economic parameter for the treatment method. It helps in elucidating the mechanism of the pollutants (AMX and CPH) removal from pollutant -loaded adsorbent, re-generation and reutilizing adsorbents, which in turn may decrease operational cost. The pollutants (AMX and CPH) desorption studies were carried out utilizing several desorption agents at the concentrations of 0.01, 0.05 and 0.1 N) including NaOH, H_2SO4, HNO_3, H_3PO_4, HCl, ethanol, acetone and water (Zhang *et al.* 2019; Hoppen *et al.* 2019). The SA-Bn-TiO_2 NPs was regenerated by 100% using water as shown in Tables 2-3.

Table 2. Comparing desorption efficiency of several type solution for the AMX onto surface of SA-Bn-TiO_2 NPs.

Regeneration and desorption (0.01 N)	E (%)	**Regeneration and desorption** (0.05 N)	E (%)	**Regeneration and desorption** (0.1 N)	E (%)
Fresh water	84.87	Fresh water	84.87	Fresh water	84.87
Ethanol	80.22	Ethanol	82.87	Ethanol	83.11
H_3PO_4	77.34	H_3PO_4	75.87	H_3PO_4	66.67
HCl	70.77	HCl	67.87	HCl	60.09
H_2SO_4	65.77	H_2SO_4	56.76	H_2SO_4	50.45
HNO_3	60.55	HNO_3	49.98	HNO_3	42.87
Methanol	55.11	Methanol	44.56	Methanol	35.01
NaOH	50.11	NaOH	42.44	NaOH	33.3

Table 3. Comparing desorption efficiency of several type solution for CPH onto surface of SA-Bn-TiO_2 NPs.

Regeneration and desorption (0.01N)	E (%)	**Regeneration and Desorption** (0.05 N)	E (%)	**Regeneration and Desorption** (0.1 N)	E (%)
Fresh water	80.29	Fresh	80.29	Fresh	80.29
Ethanol	75.12	Ethanol	78.57	Ethanol	80.11
H_3PO_4	72.76	H_3PO_4	62.87	H_3PO_4	59.99
HCl	66.87	HCl	53.87	HCl	47.09
H_2SO_4	59.98	H_2SO_4	45.98	H_2SO_4	38.87
HNO_3	50.87	HNO_3	37.87	HNO_3	30.87
Methanol	47.11	Methanol	35.55	Methanol	29.77
NaOH	44.65	NaOH	30.65	NaOH	28.98

The performance and reutilization of SA-Bn-TiO_2 NPs using water in the AMX and CPH adsorption methods were examined up to six steps under optimum conditions (Fig. 4). After 4 cycles of utilizing SA-Bn-TiO_2 NPs, the capacity was yet significant (>80%) and revealed SA-Bn-TiO_2 NPs as best adsorber (Al Bayati 2020; Sevda Pashaei Fakhri *et al.* 2021). By increasing the number of stages of hydrogel used, the capacity of hydrogel slightly decreased, which can be attributed to several parameters such as damage to active sites on the adsorbent saturation of active sites as well as breakdown of hydrogel polymer network through the continuous adsorption-de-sorption cycles which destroyed SA-Bn-TiO_2 NPs and decreased the removal capacity (Sukul *et al.* 2019; Hemant Mittal *et al.* 2021)

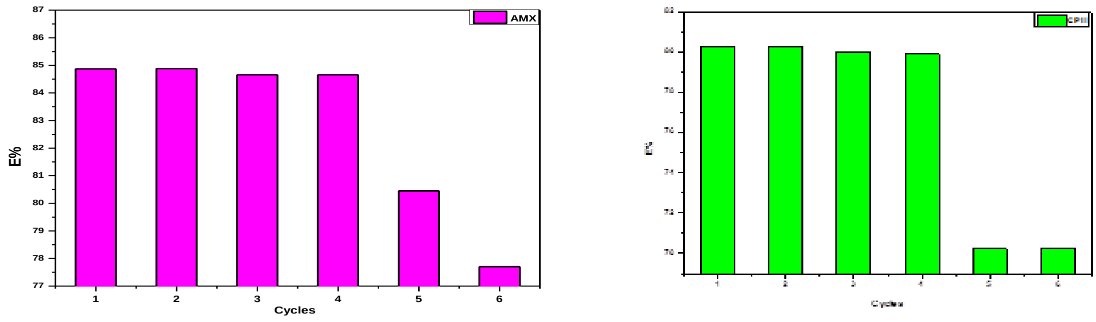

Fig. 4. multi-cycle use of SA-Bn-TiO_2 NPs for the AMX and CPH adsorption using water as desorption medium.

Kinetic models

The mechanism of adsorbate-adsorbent interaction is top described via examining the rate of expression for the adsorption dye onto SA-Bn-TiO_2 NPs. It appeared via influence of time on the adsorption method and fitting the investigational findings to several conventional models. (Abdalghaffar M Osman & Saleh 2020). The rate of expression can be estimated via analysing the adsorption result with three kinetic adsorption models: first model, second model, and Chemisorption. The fitting data are presented in Fig. 7 and Table 3. A kinetic description of adsorption (first model equation):

$$q_t=q_e[1-\exp(\ k_f\ t)] \qquad \textbf{(3)}$$

Lagergren's usability deviates from its non-linear form, according to the results. This means that the new kinetic is inadequate for forecasting first models of sorption kinetics on SA-Bn-TiO_2 NPs. We were going to apply the result to models, since the kinetic first-order failed to represent the sorption effects (Saeed *et al.* 2020). The following is an example of a second model equation calculate (Del Mar Orta *et al.* 2019; Shumei Zhao *et al.* 2020):

$$qt=\frac{\mathrm{K2qe2t}}{1+\mathrm{K2qet}} \qquad \textbf{(4)}$$

The non-linear structure of the Elovich (Chemi-sorption model) [49] as follows:

$$\mathrm{qt}=\frac{1}{\beta}1\beta\ln(\alpha\beta)+\frac{1}{\beta}\ln t \qquad (\textbf{5})$$

The kinetic adsorption from the Elovich is shown in Fig. 5 and Tables 3 - 4. The non-linear plots of qt versus t for several primary concentrations demonstrated best consistency among the experiments and determined qe values. Thus, second model of kinetic adsorption exhibited best R^2 than the Chemi-sorption model. According to results, the adsorption was better suited to second model than the Chemi-sorption model (Nasseh *et al.* 2019; Kim & Jin Hyun 2019)

Table 3. First model, second model and Elovich for the AMX and CPH adsorptions on to SA-Bn-TiO_2 NPs.

Model type	Factors	Value	Standard error	R^2
First model	qe (mg g^{-1})	84.3333	0.7577	0.9779
	kf (min^{-1})	0.0937	0.0047	
Second model	qe (mg g^{-1})	93.8769	1.0135	0.9856
	ks (gmg^{-1} min^{-1})	0.1363	0.0085	
Elovich model	α (mg g^{-1} min^{-1})	39.7754	1.9068	0.9558
	β (g min^{-1})	1.9460	0.1797	

CPH

Model type	Factors	Value	Standard error	R^2
First models	qe (mg g^{-1})	82.6858	1.4335	0.9665
	kf (min^{-1})	0.05389	0.0037	
Second model	qe (mg g^{-1})	98.253	3.5667	0.9437
	ks (gmg^{-1} min^{-1})	0.0636	0.0090	
Elovich models	α (mg g^{-1} min^{-1})	42.935	4.6214	0.8100
	β (g min^{-1})	1.4146	0.2460	

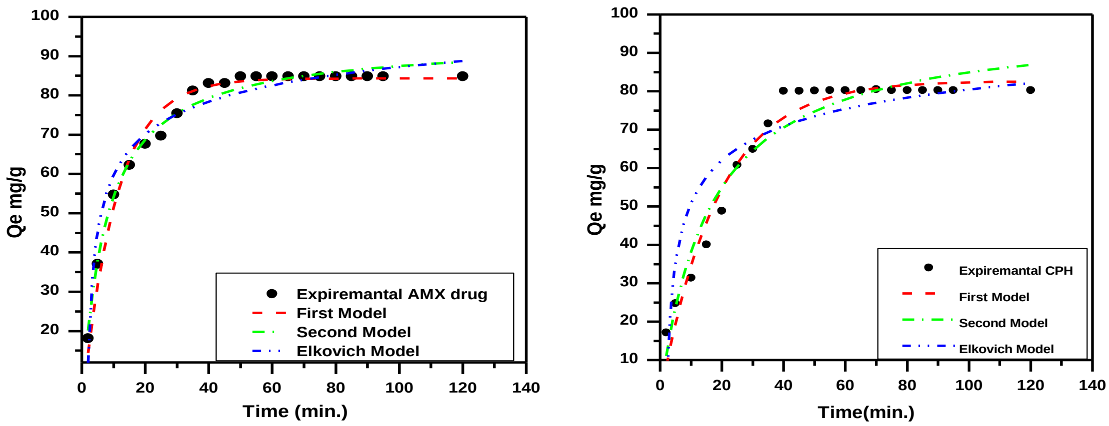

Fig. 5. Adsorption rate curve models fitted to experimental AMX and CPH onto SA-Bn-TiO_2 NPs; a) kinetic first order; b) second order; and c) Elkovich.

CONCLUSION

1. Removal of real aqueous pollutants (dyes, drugs, phenols) using SA-Bn-TiO_2 NPs to give low absorbance (0.0001) via utilizing UV-Vis spectrophotometer for at a chosen wavelength for 60 min.
2. The chemisorption, first model, and second model of kinetic were useful to test the study result. The first model exhibited the maximum fit for the kinetic models.
3. The SA-Bn-TiO_2 NPs with regeneration of 100% can be desorbed in water in the three pollutants (CR, AMX and CPH). Adsorption method was investigated up to 4 steps under optimum conditions.

REFERENCES

Abdalghaffar M Osman, AHH & Saleh, TA 2020, Simultaneous adsorption of dye and toxic metal ions using an interfacially polymerized silica/polyamide nanocomposite: Kinetic and thermodynamic studies. *Journal of Molecular Liquids*, 314: 113640.

Abdoon, FM & Yahyaa, SY 2018, Validated spectrophotometric approach for determination of salbutamol sulfate in pure and pharmaceutical dosage forms using oxidative coupling reaction. *Journal of King Saud University - Science*, 1 p., https://doi.org/10.1016/j.jksus.2018.11.002.

Abdulsada, GJ & Kadam, ZM 2019, Improvement the chemical structure, optical and magnetic properties of cufe2o4 thin films. ARPN *Journal of Engineering and Applied Sciences*, 14: 10251-10255.

Abid Alradaa, ZA & Kadam, ZM 2015, Preparation, Characterization and Prevention Biological pollution of 4 (4-Benzophenylazo) Pyrogallol and their Metal Complexes. in IOP Conference Series: Earth and Environmental Science. 2021.Alqaragully, M.B., et al., Monoethanolamine: Production plant. *Research Journal of Pharmaceutical, Biological and Chemical Sciences*, 6: 1287-1296.

Al Bayati, RA 2020, Adsorption-desorption isotherm of one of antidibetic drug from aqueous solutions on some pharmaceutical adsorbents. *European Journal of Scientific Research*, 40: 580-588.

Aljeboree, AM & Alkaim, AF 2019, Comparative removal of three textile dyes from aqueous solutions by adsorption: As a model (corn-cob source waste) of plants role in environmental enhancement. *Plant Archives*, 19: 1613-1620.

Aljeboree, AM & Alkaim, AF 2019, Role of plant wastes as an eco-friendly for pollutants (crystal violet dye) removal from aqueous solutions. *Plant Archives*, 19: 902-905.

Aljeboree, AM, Alshirifi, AN & Alkaim, AF 2019, Activated carbon (as a waste plant sources)-clay micro/nanocomposite as effective adsorbent: Process optimization for ultrasound-assisted adsorption removal of amoxicillin drug. *Plant Archives*, 19: 915-919.

Aljeboree, AM *et al.* 2019, Photocatalytic degradation of textile dye crystal violet wastewater using zinc oxide as a model of pharmaceutical threat reductions. *Journal of Global Pharma Technology*, 11: 138-143.

Al Mashhadani, ZI *et al.* 2021, Antibiotics Removal by Adsorption onto Eco-friendly Surface: Characterization and Kinetic Study. *International Journal of Pharmaceutical Quality Assurance*, 12: 252-255.

Ardizzone, S, Gabrielli, G & Lazzari, P 1993, Adsorption of methylene blue at solid/liquid and water/air interfaces. *Colloids and Surfaces A: Physicochemical and Engineering Aspects*, 76: 149-157, https://doi.org/10.1016/0927-7757(93)80073-N

Arif Chowdhury, SK, Ahmad Khan, A, Ravi Chandra, M & Hussain, SH 2020, Activated carbon loaded with Ni-Co-S nanoparticle for Superior Adsorption Capacity of Antibiotics and Dye from Wastewater: Kinetics and Isotherms. *Journal Pre-proof*, https://doi.org/10.1016/j.colsurfa.2020.125868.

Ashour, S & Bayram, R 2019, Selective and validated kinetic spectrophotometric method for the determination of irbesartan in pure and pharmaceutical formulations. *Annales Pharmaceutiques Fran§aises*, 77: 101-111.

Bader, AT et al., Removal of Methyl Violet (MV) from aqueous solutions by adsorption using activated carbon from pine husks (plant waste sources). *Plant Archives*, 19: 898-901.

Del Mar Orta, M, Martin, J, Medina Carrasco, S, Santos, JL, Aparicio, I & Alonso, E 2019, Adsorption of propranolol onto montmorillonite: Kinetic, isotherm and pH studies. *Applied Clay Science*, 173: 107-114.

Hemant Mittal, AAA, Morajkar, PP & Alhassan, SM 2021, Graphene oxide crosslinked hydrogel nanocomposites of xanthan gum for the adsorption of crystal violet dye. *Journal of Molecular Liquids*, 323: 115034.

Ho, Y & McKay, G 1998, A comparison of chemisorption kinetic models applied to pollutant removal on various sorbents. *Process Safety and Environmental Protection*, 76: 332-340.

Hoppen, MI, Carvalho, KQ, Ferreira, RC, Passig, FH, Pereira, IC, Rizzo Domingues, RCP, Lenzi, MK & Bottini, RCR 2019, Adsorption and desorption of acetylsalicylic acid onto activated carbon of babassu coconut mesocarp. *Journal of Environmental Chemical Engineering*, 7: 102862.

Karim, AR & Radia, ND 2022, Hydrogel/clay nanocomposites for removal of cationic organic dye from their aqueous solutions. *HIV Nursing*, 22: 1936-1940.

Karim, AR & Radia, ND 2022, Synthesis and Characterization of Sodium Alginate-G-Poly (AAC-AAM)/BC Nanocomposite Hydrogel and its Application for Dyes Adsorption. *HIV Nursing*, 22: 1945-1949.

Kim, YS & Jin Hyun, K 2019, Isotherm, kinetic and thermodynamic studies on the adsorption of paclitaxel onto Sylopute. *The Journal of Chemical Thermodynamics*, 130: 104-113.

Metrani, R, Jayaprakasha, GK & Patil, BS 2018, Optimized method for the quantification of pyruvic acid in onions by microplate reader and confirmation by high resolution mass spectra. *Food Chemistry*, 242: 451-458.

Nasseh, N, Barikbin, B, Taghavi, L & Nasseri, MA 2019, Adsorption of metronidazole antibiotic using a new magnetic nanocomposite from simulated wastewater (isotherm, kinetic and thermodynamic studies). *Composites Part B*: *Engineering*, 159: 146-156.

Nasir, ZA, Swadi Tlaiaa, Y, Hassoon Ali, A 2022, Design of dissolved air flotation (DAF) process for treating dyescontaminated wastewater. *Caspian Journal of Environmental Sciences*, 20: 315-322.

Rangaraju, A & Chaitanya, K 2018, Spectrophotometric determination of lamotrignine using oxidative coupling reaction in Pharmaceutical dosage forms. *Journal of Innovation in Pharmaceutical Sciences*, 2: 49-52.

Rouquerol, F, Rouquerol, J & Sing, K 1999, Adsorption by powders and porous solids. Academic Press, London. Adsorption by powders and porous solids. Academic Press, London, eBook ISBN: 9780080526010.

Saleh Ibrahim, A, Chyad Al-Hamadani, R, F, Fahim Chyad, T, H. Ali, S 2022, Using ozone for activation of manufactured porous media to improve the removal efficiency of heavy metals from industrial wastewater. *Caspian Journal of Environmental Sciences*, 20: 283-294.

Saeed, UJ, Adnan, AK, Saad, M, Iftikhar, A, Guohua, S, Cheng Meng, C & Rashid, A 2020, Removal of azo dye from aqueous solution by a low-cost activated carbon prepared from coal: adsorption kinetics, isotherms study, and DFT simulation. *Environmental Science and Pollution Research*, 28:10234-10247, DOI: 10.1007/s11356-020-11344-4.

Sevda Pashaei Fakhri, SJP, Foroutan, R, Arsalani, N & Ramavandi, B 2021, Crystal violet dye sorption over acrylamide/graphene oxide bonded sodium alginate nanocomposite hydrogel *Chemosphere*, 270: 129419.

Shoaib Nawa , MS, Khan, R, Riaz, N, Waheed ,U, Shahzadi, I & Ali, A 2022, Ultrasound-Assisted Hydrogen Peroxide and Iron Sulfate Mediated Fenton Process as an Efficient Advanced Oxidation Process for the Removal of Congo Red Dye. *Polish Journal of Environmental Studies*, 31: 1-13.

Shumei Zhao, YZ, Wan, X, He, Sh, Yang, X, Hu, J & Zhang, G 2020, Selective and efficient adsorption of anionic dyes by core/shell magnetic MWCNTs nano-hybrid constructed through facial polydopamine tailored graft polymerization: Insight of adsorption mechanism, kinetic, isotherm and thermodynamic study. *Journal of Molecular Liquids*, 319: 1-6.

Sukul, P, Lamsh, M, Zhlke, S & Spiteller, M S 2019, Michael Sorption and desorption of sulfadiazine in soil and soil-manure systems. *Chemosphere*, 73: 1344-1350.

Wared, SHH & Radia, ND 2020, Synthesis and characterization of sodium alginate-g-polyacrylic acid hydrogel and its application for crystal violet dye adsorption. *International Journal of Drug Delivery Technology*, 11: 556-565.

Xiong, J *et al.* 2020, Hexagonal boron nitride adsorbent: Synthesis, performance tailoring and applications. *Journal of Energy Chemistry*, 40: 99-111.

Zhang, G, Feizbakhshan, M, Zheng, Sh, Hashisho, Z, Sun, Z, Yangyu, L 2019, Effects of properties of minerals adsorbents for the adsorption and desorption of volatile organic compounds (VOC). *Applied Clay Science*, 173: 88-96.

Bibliographic information of this paper for citing:

Alhattab, ZD, Aljeboree, AM, Jawad, MA, Sheri, FS, Obaid Aldulaim, AK, Alkaim, AF 2023, Highly adsorption of alginate/bentonite impregnated TiO_2 beads for wastewater treatment: Optimization, kinetics, and regeneration studies. Caspian Journal of Environmental Sciences, 21: 657-664.